

## DEBRIS AND METEOROID PROPORTIONS DEDUCED FROM IMPACT CRATER RESIDUE ANALYSIS

Lucinda Berthoud  
Jean-Claude Mandeville  
CERT-ONERA / DERTS  
2, Avenue E.Belin, 31055 Toulouse Cedex (France)  
Phone: (33) 61557117, Fax (33) 61557169

238-90  
14F

Christian Durin  
CNES RA-DP EQ/QM  
18, Avenue E.Belin, 31055 Toulouse Cedex (France)  
Phone: (33) 61281439, Fax (33) 61274732

Janet Borg  
Institut d'Astrophysique Spatiale  
Bat 121, 91405 Orsay Cedex, (France)  
Phone: (33) 1 6985 8632, Fax: (33) 1 6985 8675

### ABSTRACT

This study is a further investigation of space-exposed samples recovered from the LDEF satellite and the Franco-Russian 'Aragatz' dust collection experiment on the Mir Space Station. Impact craters with diameters ranging from 1 to 900  $\mu\text{m}$  were found on the retrieved samples. Elemental analysis of residues found in the impact craters was carried out using Energy Dispersive X-ray spectrometry (EDX). The analyses show evidence of micrometeoroid and orbital debris origins for the impacts. The proportions of these two components vary according to particle size and experiment position with respect to the leading edge of the spacecraft. On the LDEF leading edge 17% of the impacts were apparently caused by micrometeoroids and 11% by debris; on the LDEF trailing edge 23% of the impacts are apparently caused by micrometeoroids and 4% consist of debris particles - mostly larger than 3  $\mu\text{m}$  in diameter - in elliptical orbits around the Earth. For Mir, the analyses indicate that micrometeoroids form 23% of impacts and debris 9%. However, we note that 60-70% of the craters are unidentifiable, so the definitive proportions of natural v. man-made particles are yet to be determined.

Experiments carried out using a light gas gun to accelerate glass spheres and fragments demonstrate the influence of particle shape on crater morphology. The experiments also show that it is more difficult to analyse the residues produced by an irregular fragment than those produced by a spherical projectile. If the particle is travelling above a certain velocity, it vapourises upon impact and no residues are left. Simulation experiments carried out with an electrostatic accelerator indicate that this limit is about 14 km/s for Fe particles impacting Al targets. This chemical analysis cut-off may bias interpretations of the relative populations of meteoroid and orbital debris. Oblique impacts and multiple foil detectors provide a higher likelihood of detection of residues as the velocities involved are lower.

### 1. INTRODUCTION

One of the objectives of retrievable experiments flown in LEO is the identification of the particles responsible for the formation of craters. This identification is achieved by chemical analysis of particle remnants or residues in and around the crater. In this work, the analysis of a number of craters on various experimental surfaces allows a statistical evaluation of the relative proportions of

meteoroids and orbital debris. The results from the LDEF and Mir experiments will contribute to an assessment of the evolution of these two populations and their origins.

However, the interpretation of impact craters is complicated by the large variety of particles in terms of their composition, shapes, orbits and velocities. This study examines the effect of particle shape and velocity on crater morphology and the possibility of EDX detection of particle residues.

## 2. EXPERIMENTS TO INVESTIGATE THE INFLUENCE OF VELOCITY

The aim of these experiments was to investigate the effect of velocity on the quantity and form of the remnants in the craters after impact. The idea was to compare the morphology and form of the residues in the simulated impacts with those found in the space-exposed samples. Similar experiments have previously been performed by Mandeville for polystyrene impacting glass targets (1). Our surfaces flown on LDEF and Mir consisted principally of 99% pure Al foils (chosen as the behaviour of Al under impact is well known) and the majority of craters analysed were  $\mu\text{m}$  in diameter. In order to simulate these conditions,  $\mu\text{m}$ -sized Fe projectiles were accelerated by a 2MV electrostatic accelerator onto the same Al foils. The accelerator facilities were provided by the Max Planck Institut für Kernphysik in Heidelberg. The tests were conducted at 1, 3, 5.5, 8, 10, 12 and 14 km/s.

Figure 1 shows scanning electron microscope (SEM) images for typical craters produced at each velocity. A corresponding elemental analysis spectrum of the remnants was produced for each crater, using an Energy Dispersive X-ray spectrometer (EDX). The images show the evolution of the form of the remnants with increasing velocity. The particle changes from intact (for 1 and 3 km/s) through fragmented (5.5 km/s), both giving strong Fe signals on the EDX spectra, to a thin molten layer where Fe is still detectable (at 8 to 10 km/s) and finally to an invisible vapourised layer where detection becomes more difficult (14 km/s). From these experiments it appears that the velocity limit for Fe particles impacting on aluminium for our EDX detection lies just above 14 km/s.

## 3. EXPERIMENTS TO INVESTIGATE THE INFLUENCE OF PARTICLE SHAPE

These experiments were carried out using the 5 mm calibre light gas gun at the hypervelocity gun laboratory run by Dr Friedrich Hörz at NASA Johnson Space Center. Six impacts using spheres (diameter 150  $\mu\text{m}$ ) and seven impacts using fragments (nominally the same diameter) of soda lime glass were fired at approximately 6 km/s onto thick targets of 6061-T6 aluminium (figure 2). The soda lime glass contains  $\text{SiO}_2$ ,  $\text{MgO}$ ,  $\text{K}_2\text{O}$ ,  $\text{Na}_2\text{O}$  and  $\text{CaO}$  whose presence or absence in the residues give clues to the vapour-fractionation processes during impact.

The sphere craters show considerable symmetry and uniformity in the crater bottom and lip thickness. The glass is in a melt form, pancaking over the bottom of the crater, then breaking up from the centre (figure 3) and 'walking' up the walls. Below the SEM image is a typical EDX spectrum of a sphere crater melt. EDX analysis of the glass melt revealed a strong presence of Al, Si, O, Na, Ca and some Mg. No K was detected, although this was not surprising as K is the most volatile component of the glass.

For the fragment craters, the general morphology was highly irregular (figure 4). The crater bottoms showed shelves and pockets of different depths. This type of irregular geometry was also seen in the larger impact craters on LDEF samples. EDX analyses (see spectrum under SEM image) indicated a strong presence of Al, Si, O and Na, but significantly less Ca and Mg than for the sphere craters, and again no K was found. These results are consistent with the relative volatility of the various elements. It is apparently more difficult to detect residues in craters formed by irregularly shaped projectiles. This may be because the layer of residue is thinner, being spread over a larger crater surface area, or that more of the projectile has been ejected.

Even though particles may be travelling at velocities  $< 10$  km/s, where one would expect to find residues, their irregular shape may prejudice EDX detection of residues. The high proportion of craters with no identifiable residues found on space-exposed surfaces may therefore be partly due to impacts by particles of irregular shape.

#### 4. OBSERVATIONS OF CRATERS ON EXPOSED SAMPLES

##### Crater Forms

Three different forms of micron-sized craters were observed on an aluminium target on the trailing edge of LDEF (reference no.: A54). FESEM images of the three different types are shown in [figure 5](#). Craters of type 'a' are very shallow with small, sometimes nonexistent rims. Craters of type 'b' are also shallow and show a crystalline structure. Craters of type 'c' are typical of the result of a hypervelocity impact with products of fusion on crater bottom, lips and even outside. In 15 out of 17 impacts with diameters 1-7  $\mu\text{m}$ , residues compatible with a micrometeoroid origin were found. The rest of our analyses were performed exclusively on craters of type 'c', as these were most easily distinguishable from material defects, and very few types 'a' and 'b' were seen for the larger craters. However, the FESEM possesses a higher resolution than a normal SEM and therefore allows distinction for craters down to almost submicron levels. It is possible that craters of types 'a' and 'b' have been created by low density or low velocity particles. This requires further investigation.

##### Residue Forms

Craters on LDEF and Mir surfaces show various states of impact melt. Craters full of solid projectile residue or with unmelted fragments were rare. More frequently impact melt was found in the form of smooth flows of material culminating in droplets. The flows of material have been seen to take serpentine forms in crater bottoms, to stop halfway up the crater walls and to leave signs of fusion out as far as the crater lips. Experiments show that the progression between these states is a function of impactor velocity: the melt appears to 'walk' up the crater walls with increasing velocity. The smallest craters observed were more likely to show signs of fusion on their lips, whereas the larger craters showed most droplets remaining at the crater bottom. The movement of the melt up the wall does not also seem to be a function of impactor size and could perhaps therefore serve as an indicator of impact velocity.

#### 5. ANALYSIS OF CRATER RESIDUES

A Link EDX analyser and a Jeol 840A SEM were used to carry out elemental analysis of impact features on various LDEF and Mir experimental surfaces. Backscattering electron images and spot analyses in and around the crater were made in the search for particle remnants. It was found necessary to tilt the sample toward the detector ( $20^\circ$ -  $40^\circ$ ) for large craters in order to avoid a shadowing phenomenon. Long detection times (up to 3000s) were used when a very thin vapourisation layer was suspected. Contaminants deposited at low velocities on the target surface were sometimes easy to identify because of their shape. However, to be absolutely sure, any particle just resting inside a crater, not an integral part of the crater interior, was considered a contaminant. A brief survey of contaminants deposited on the surface of the LDEF clamps revealed glass and carbon fibres released by the atomic oxygen reduction of their matrices, paint flakes (similarly released), salt crystals, silica, spheres of FeO (probably manufacturing debris), gas phase elements which have recrystallised onto the surface and human residues (fingerprints and hairs). Non-aluminium phases inherent within alloy targets were taken into account by systematically performing an analysis of the

experimental surface outside the crater area. In this way, if clumps of the same elements were found both inside and outside the crater they were considered to be inclusions.

The following guidelines were used in the identification of meteoroids (based on analyses of interplanetary dust particles) and debris (based on analyses of craters found on Skylab, Shuttle windows and Solar Max) (2):

*Meteoroids:*

- Fe-S-Ni : High Fe content with smaller proportions of S and Ni
- Mafic silicates : Varying proportions of Mg, Fe, Si, Ca with possible Al, S, Ni
- Chondrites : High Si content with smaller proportions of Mg, Ca and Fe.

*Debris:*

- Al : Al with smaller proportions of O and trace elements
- Steels : Fe with smaller proportions of Mg, Si, Cd, Ti, V, Cr, Ni, Mn, Co, Cu, Zn
- Al<sub>2</sub>O<sub>3</sub> from solid rocket fuel : Al and O
- Paint flakes : Ti, Si and Zn
- Alloys : Different proportions of Ca, Si, Ti, K, Zn, Co, Sn, Pb, Cu, S, Cl, Au or Ag.

**5.1. LDEF Trailing Edge Results from FRECOPA (row O3)**

The French experiment FRECOPA was located on the trailing edge (row O3) of the Long Duration Exposure Facility (LDEF). It was thought that this position would ensure that 100% of the impacts were caused by micrometeoroids, assuming that orbital debris are in circular orbits. Residues were found in craters as small as 1 µm and as large as 250 µm. 49 craters were analysed and the results can be broken down into size categories as follows:

Table 1 : Results of chemical analysis of FRECOPA

Crater size in µm	1 < D < 200	1 < D < 15	15 < D < 100	D > 100
Debris	4%	8%	9%	0%
Meteoroid	23%	29%	18%	25%
Unknown	73%	63%	73%	75%

In comparison, Hörz and Bernhard (3) have analysed 187 craters 10-900 µm in diameter on gold samples on the CME experiment (tray A03). Their findings are resumed along with all the meteoroid/debris proportions that we have found for the different experimental surfaces in table 2.

An example of an impact caused by a natural particle found on FRECOPA ER 3-8 is seen in figure 6. The ellipticity and shallowness of the crater (P/D=0.3) indicate an oblique impact. The low normal component of the velocity was apparently not sufficient to cause complete melting or vapourisation of the impactor. The residues are seen to be partly unmelted fragments and partly melted droplets. EDX analysis (see spectrum) of the melt residues reveal a micrometeoroid signature, with the presence of Al, Mg, Si, Fe, O, S, Ca and Cr.

The discovery of orbital debris impacts on the trailing edge is particularly significant as it confirms the presence of debris in elliptical orbits around the Earth (2). The impacts showed evidence of stainless steel and paint flake impactors. An example of an impact on sample A5 is shown in figure 7. The impactor is still intact, although slightly fractured, and from the shape of the

crater we deduce that the impact was oblique and of low velocity. EDX analysis of the residues shows the presence of Al (the substrate), Fe, V and Cr, indicating a steel origin.

### 5.2. LDEF Leading Edge (row 09) from MAP and clamps

The University of Kent at Canterbury supplied us with samples of 25 µm thick aluminium bonded to a gold-plated brass mesh from the Micro Abrasion Package (MAP) mounted on the leading edge of LDEF (4). However, for the MAP surfaces, no evidence of impact particule residues was found. A high level of impurities/inclusions within the aluminium alloy made analysis extremely difficult.

The LDEF clamps, consisting of plates of 6061-T6 Al, were used to fix experiment trays to the LDEF frame. This alloy also contains the elements Mg, Si, Fe and Cr, which sometimes appear as inclusions of Mg<sub>2</sub>Si, AlCrMg and FeAlSi. These inclusions are easily recognizable in a scanning electron microscope from their characteristic forms, so that confusion with extra-terrestrial matter is unlikely. 35 craters with diameters ranging from 60 µm to 900 µm were analysed for the clamps on rows 08 and row 09. For these craters > 50 µm, 11% showed evidence of debris origin, 17% showed evidence of meteoroid origin and 72% were of unknown origin. Figure 8 shows an impact apparently of low velocity onto clamp A06 C06. Unmelted fragments are clearly visible inside the crater. EDX spectra of different areas of the fragments show a wide range of proportions of the elements Al, Mg, Si, Ca, Fe and Cr frequently found in micrometeoroids (see W7027F11 in the Cosmic Dust Catalog for a comparison (5)) revealing the particle's agglomerate nature and similarity to certain chondritic interplanetary dust particles.

### 5.3. MIR Results from ARAGATZ experiment

The MIR Space Station has been in orbit at an altitude of 350-450 km, inclination 51.6° since February 1986. The French experiment module 'Echantillons' was mounted on the side of the Mir core module on the 9th December 1988 and recovered on the 11th of January 1990. The experiment module consisted of a 1 x 1 x 0.2 m frame supporting five experiments. Two of the experiments consisting of aluminium target surfaces were designed to study the composition and distribution of dust particles in Low Earth Orbit (6).

From the analysis of 65 craters ranging in diameter from 1-200 µm (but mainly 1-10 µm), 68% show no residues, 23% are consistent with natural particle elements and 9% show evidence of orbital debris impact. The debris appear to be principally of glass and flakes of paint.

A summary of the results of analyses carried out during this work is given in table 2.

Table 2.

Surface	Material	Crater D	% met	% debris	% unknown
LDEF09	Al	50-600 µm	17	11	72
LDEF03	Al	1-200 µm	23	4	73
LDEF03	Au*	10-900 µm	30	15 (Al incl.)	55
Mir	Al	1-200 µm	23	9	68

\* Analyses carried out by Bernhard, Hörz on gold samples from CME expt. (3)

#### 5.4. Multiple Foil Detectors

Multiple foil detectors were used on Mir and on LDEF. Several chemically interesting impact features on the multiple foil detectors were observed. The thin upper foil apparently slows and fragments the impacting particle, causing secondary craters on the capture surface beneath. The fragments are then easily analysed.

### 6. DISCUSSION

EDX analysis can only identify elements if significant amounts are present ( $> 0.2-0.5\%$  of weight analysed). Quantitative analysis inside craters is fraught with problems and EDX is not suited to identifying thin melt or vapour layers, as it analyses a pear-shaped volume. But, being quick and reliable, it does provide an excellent tool in the initial search for residues. Unlike for SIMS, crater shadowing problems with EDX can be solved simply by tilting and rotating the sample. Once the residues have been identified as natural or man-made and extracted from the crater, a more precise analysis technique can be applied (such as ion microprobe or TEM).

The high proportions of craters of unidentified origins are due partly to our aluminium detecting surfaces which preclude the identification of aluminium particles. Hörz and Bernhard found that of the debris they detected, 83% were aluminium-based. They consequently found lower levels of unidentified craters (55% compared to our 70%). Another factor contributing to the proportion of unidentified craters is the velocity of impact. Our acceleration experiments show that if the impact velocity is higher than a certain limit, a large percentage of the particle will be vapourised, leaving a thin layer of melt undetectable using EDX methods. This will happen at lower velocities for the more volatile elements and for heterogeneous particles which may blow apart under impact pressures. Our experiments indicate that the shape of the projectile also plays a part in identification of residues. It was found more difficult to detect the residues of an irregularly shaped particle than those of a spherical particle.

Meteoroid impact velocities on LDEF vary between 16.7 km/s (trailing edge) and 23.2 km/s (leading edge). For Mir the velocities are between 14.5 and 29.8 km/s, depending on the position in orbit (7). Considering these velocities, it is surprising that we have been able to detect residues of meteoroids at all. However, this may be linked to the oblique impacts of a proportion of the particles. In this work we have found that oblique impacts increase the likelihood of finding residues in craters, because they effectively mean a lower normal component of velocity. On LDEF the proportions of oblique impacts found were 3% for the leading edge and 10% for the trailing edge. For Mir the proportions were higher at 10-20% (for a further discussion of this see (8)).

The presence of debris on the trailing edge of LDEF requires an explanation. Previously debris were thought to move uniquely in circular orbits around the Earth. However, these results in conjunction with the higher flux measured on the trailing edge as compared with Grün's meteoroid model implies otherwise. It is possible that debris are also to be found in non-bound orbits or alternatively in elliptical orbits around the Earth (2). Orbital calculations show that it is possible for debris in Geostationary Transfer Orbit to strike the trailing edge of LDEF with a velocity of 2-3 km/s.

### 7. CONCLUSIONS

The aim of this investigation was to determine the proportions of debris and meteoroids in Low Earth Orbit. This was achieved by analysing particle residues left in hypervelocity impact craters on LDEF and Mir surfaces using EDX. However, no residues could be detected in a large

proportion of the craters. Acceleration experiments on a micron scale were carried out to investigate the influence of impact velocity and particle shape on the eventual form of the residues.

Laboratory acceleration experiments have shown that impact velocity and particle shape determines the possibility of residue detection in craters. It was found more difficult to detect residues in craters produced by irregularly-shaped particles, than those in craters produced by spherical particles. The limit for detection for Fe particles impacting Al is around 14 km/s. Above this velocity, the particle is significantly melted and vapourised. Chemical identification of residues is therefore easier for low velocity impacts. This means that oblique impacts and multiple foil detectors, which both slow down the impacting particle, are more likely to show residues than normal impacts onto semi-infinite targets. It also means that the analysis results are biased towards orbital debris, as these travel at lower velocities than micrometeoroids.

We propose that the high percentage of unidentified craters is due to aluminium impactors (undetectable on our aluminium collecting surfaces), the vapourisation of the particles due to high impact velocities, and to their irregular shape.

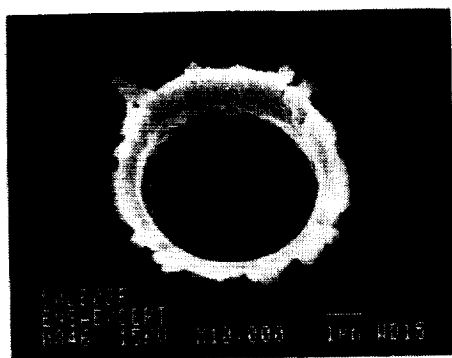
## 8. ACKNOWLEDGEMENTS

The authors would like to express their thanks to Dr Friedrich Hörz and members of the Hypervelocity Gun Laboratory at NASA JSC in Houston for carrying out acceleration tests; equally to Professor Eberhard Grün and dept. of the MPI für Kernphysik, Heidelberg for providing accelerator facilities, to Dr Michael Zolensky at NASA JSC, Ronald Bernhard and Jack Warren of Lockheed ESC/JSC for providing the LDEF clamps, and to Professor Tony McDonnell at the Univ. of Kent, Canterbury for LDEF MAP samples. This work was partly supported by a European Commission research grant under the 'Science' programme.

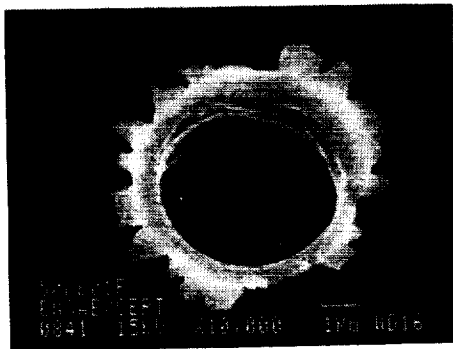
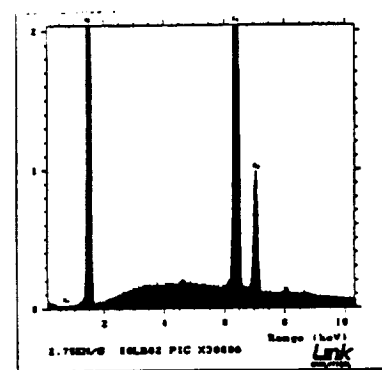
## 9. REFERENCES

- (1) Mandeville J.C., Vedder J.F. (1971) "Microcraters formed in glass by low density projectiles", *Earth and Planet. Sci. Letters*, Vol.11, No.4.
- (2) Zolensky M.E. et al. (1992): "Interim report of the Meteoroid and Debris Special Investigation Group", Part 2 of '*LDEF-Second Post-Retrieval Symposium*', NASA Conf. Publ. 3194, pp 277.
- (3) Hörz F., Bernhard R.P. (1992) "Compositional analysis and classification of projectile residues in LDEF impact craters"*NASA TM-104750*.
- (4) McDonnell, J.A.M. (1984) "Multiple Foil Microabrasion Package" in '*LDEF Mission 1 Experiments*', eds. L.G. Clark, W.H. Kinard et al. NASA SP-473, pp 117-120.
- (5) NASA Cosmic Dust catalog (1983) Vol.4, No. 2, *NASA Pub. 65*, JSC 18928.
- (6) Mandeville J.C. (1990) "Aragatz mission dust collection experiment", *Adv. Space Research* Vol. 10, No. 3-4, pp. 397-401.
- (7) Mandeville J.C. and Berthoud L. (1993) "Micrometeoroids and debris on LDEF", '*LDEF-Third Post-Retrieval Symposium*' (this volume).
- (8) Berthoud L. (1993) "Micrometeoroids and orbital debris observed in low earth orbit (LEO)," PhD thesis, Ecole Nationale Supérieure de l'Aéronautique et de l'Espace, Toulouse, France.

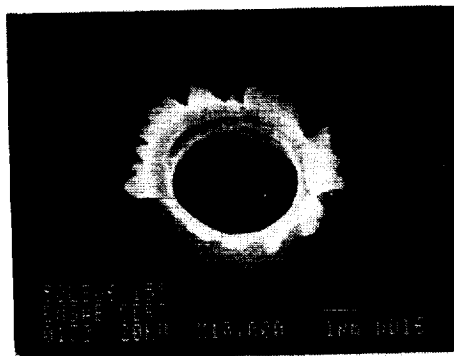
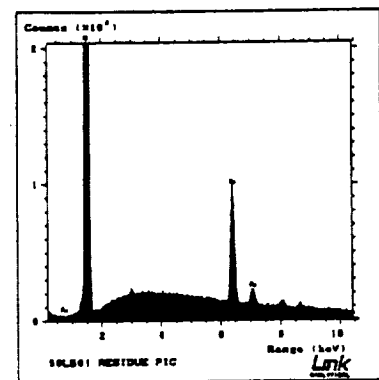
Figure 1: SEM images and EDX analyses of Fe residues in craters for increasing impact velocities ( $\mu\text{m}$  Fe particles accelerated onto 99% pure Al targets)



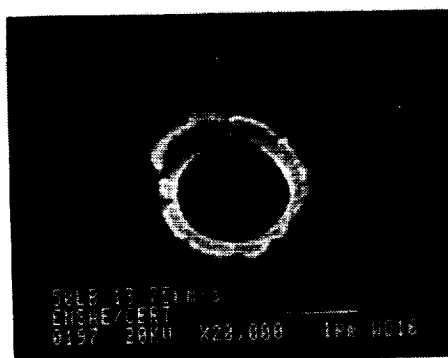
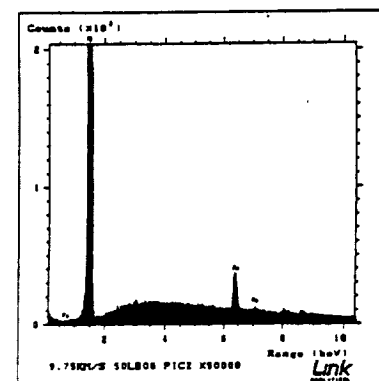
3 km/s



5.5 km/s



10 km/s



14 km/s

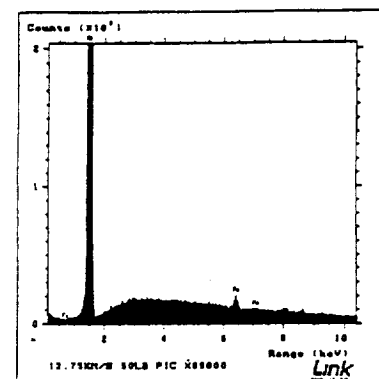


Figure 2: Soda lime glass spheres (diameter 150  $\mu\text{m}$ ) and fragments used as projectiles in particle shape simulation experiments (samples provided by NASA JSC)

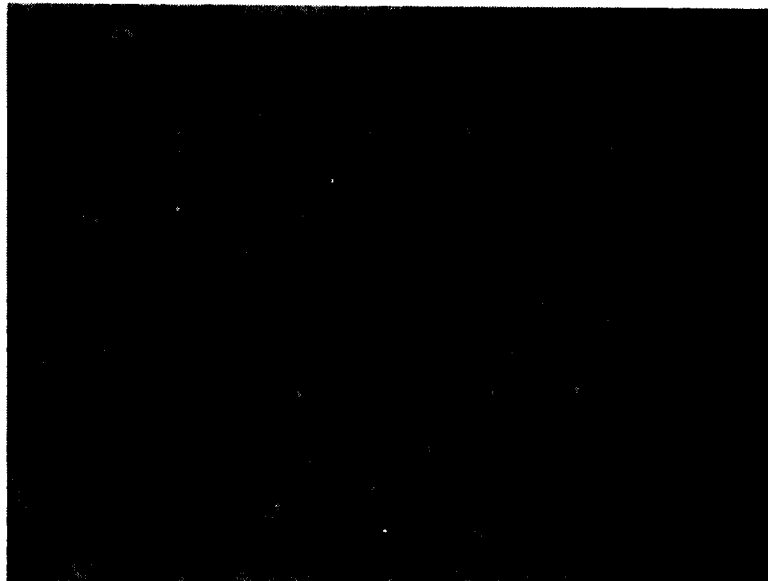


Figure 3: Glass melt from spherical projectile in crater in aluminium target 1217B ( $D = 450 \mu\text{m}$ ). Experiments carried out at Hypervelocity Gun Lab. NASA, JSC.

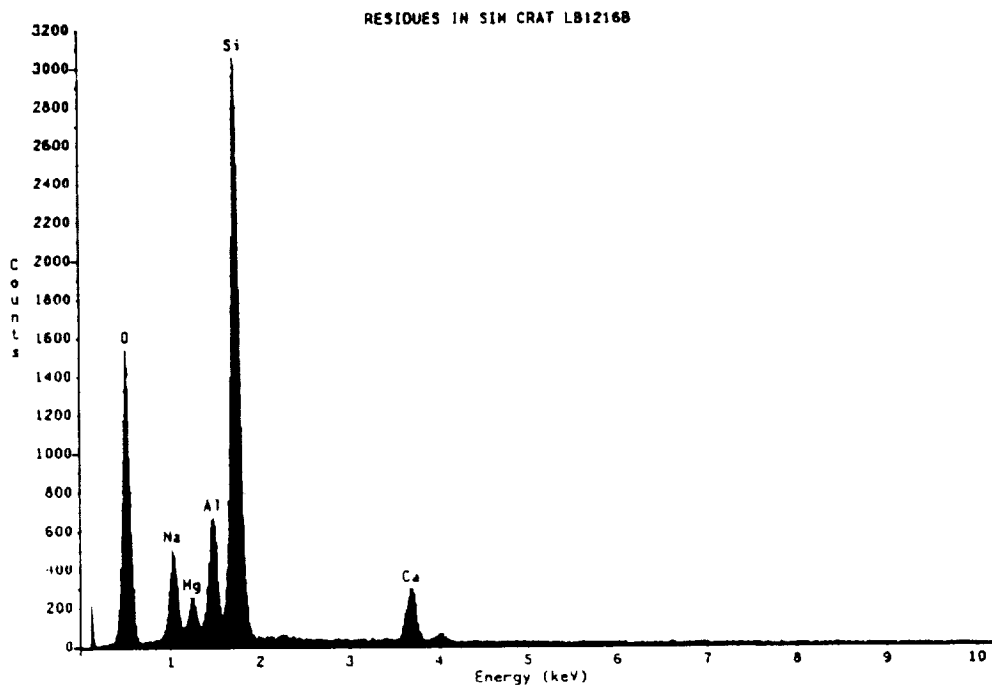
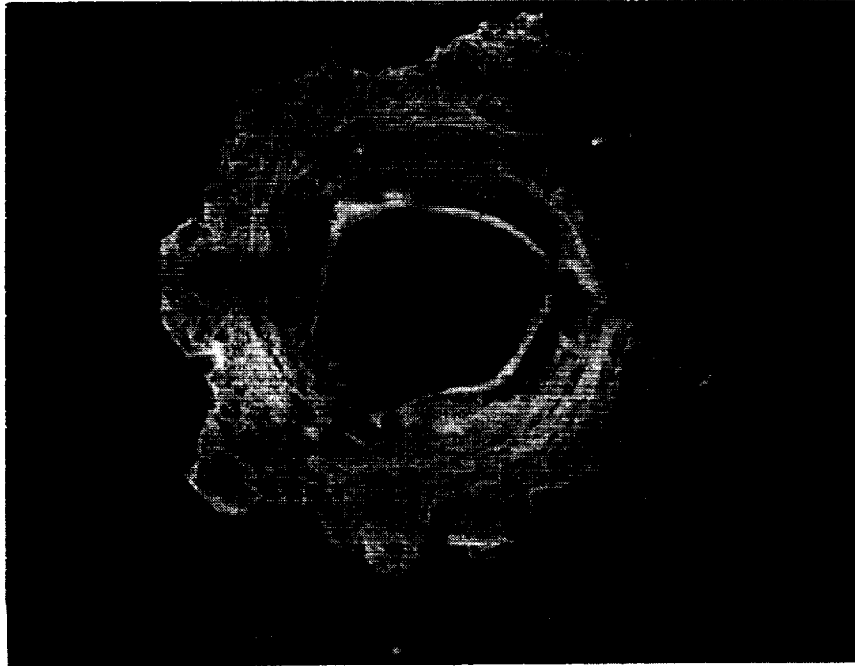


Figure 4: Crater from fragment of glass impact in aluminium target 1225B (D = 235  $\mu\text{m}$ ).  
Experiments carried out at Hypervelocity Gun Lab. NASA, JSC.

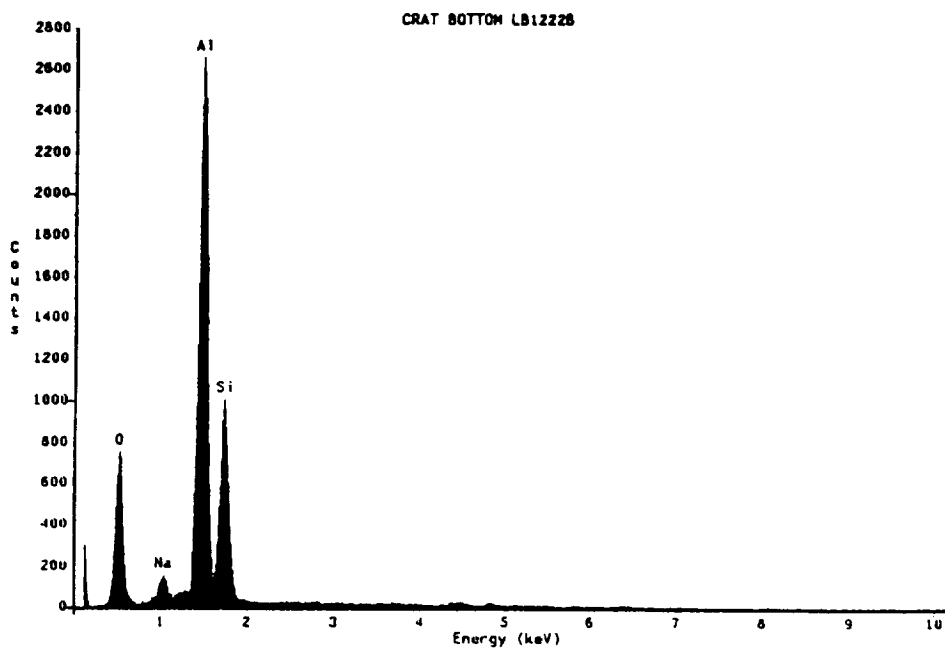


Figure 5: (Janet Borg)

**FRECOPA TRAY : A0138-1 experiment**  
typical micron-sized craters in A54 Al target

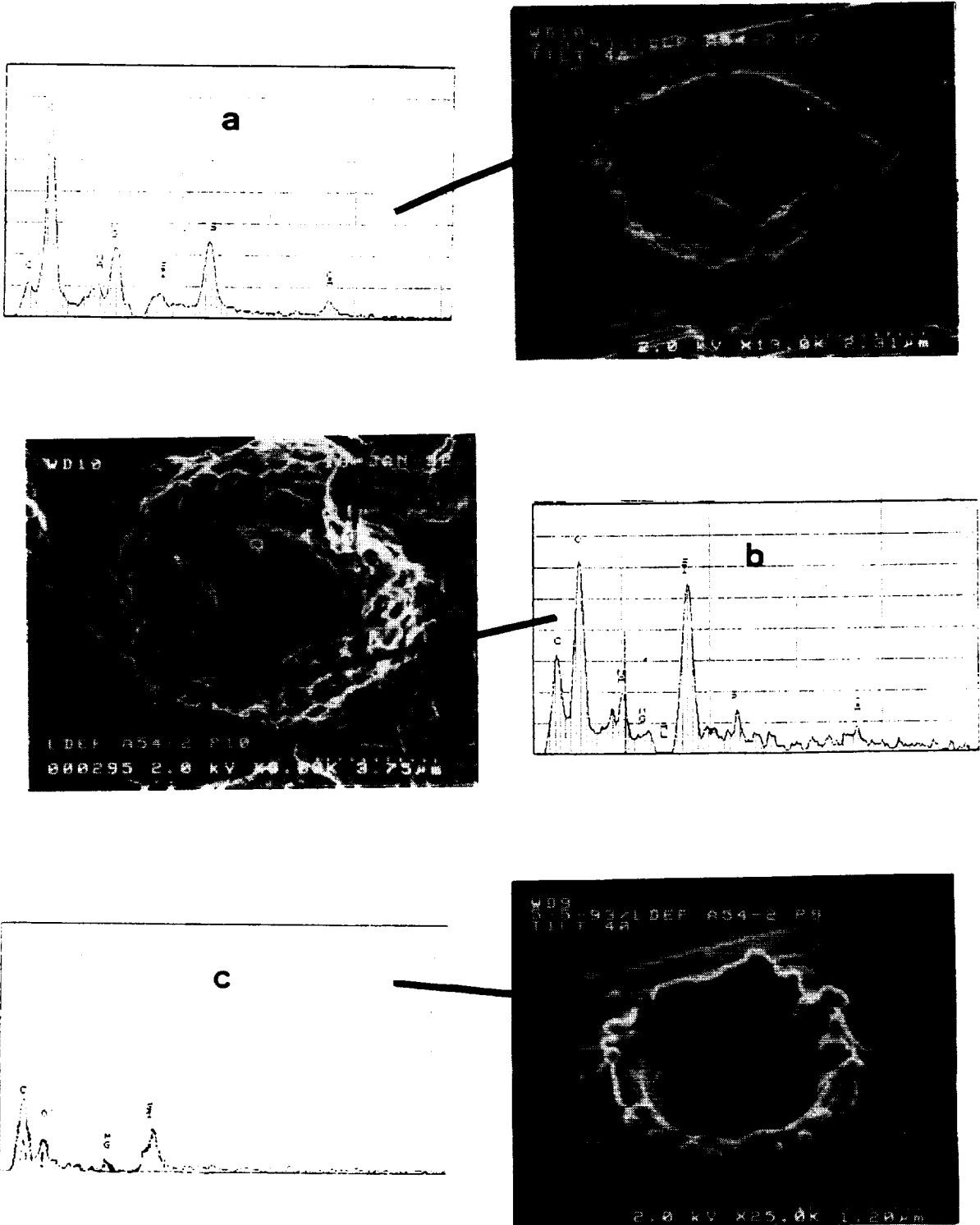


Figure 6: Meteoroid impact on LDEF FRECOPA (03) 'Ecran Rigide'.

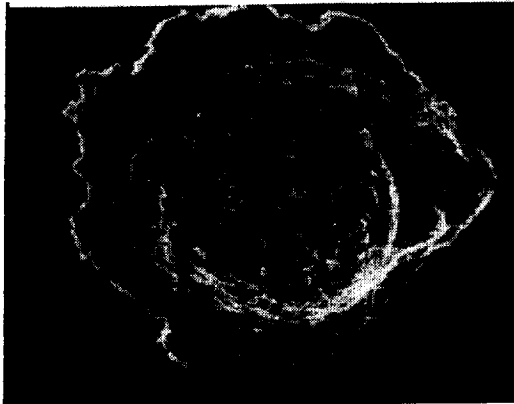


Figure a: Oblique impact (235 x 176 μm) on Al alloy experiment support surface.

Figure 7: Debris impact on LDEF FRECOPA.

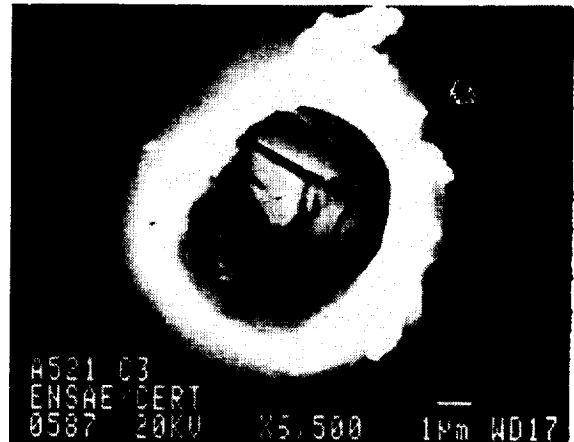


Figure a: Oblique impact (6.6 x 5.4 μm) on 99% pure Al experiment surface.



Figure b: Detail showing molten residues.

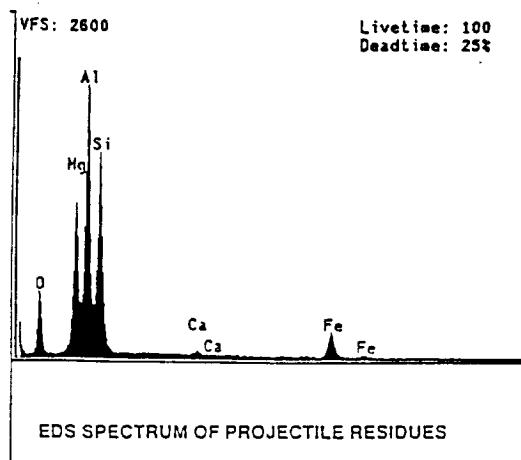


Figure c: EDS spectrum of residues (15 keV).

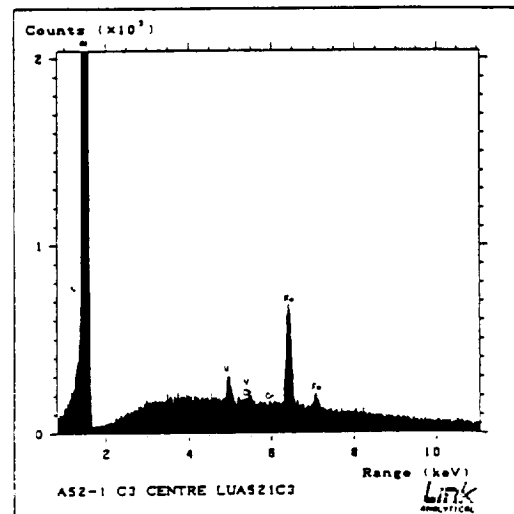


Figure c: EDS spectrum of figure 5a residues (20 keV).

Figure 8: Low velocity impact (33  $\mu\text{m}$ ) in LDEF clamp A06C06 with spectra from different areas of the residues to show different grain compositions.

